Since January 2020 Elsevier has created a COVID-19 resource centre with free information in English and Mandarin on the novel coronavirus COVID-19. The COVID-19 resource centre is hosted on Elsevier Connect, the company's public news and information website.

Virology 390 (2009) 79–88

Contents lists available at ScienceDirect

Virology

journal homepage: www.elsevier.com/locate/yviro

Homologous genetic recombination in the yellow head complex of nidoviruses infecting *Penaeus monodon* shrimp

Priyanjalie K.M. Wijegoonawardane [a,1], Nusra Sittidilokratna [b,c,d], Natthida Petchampai [d], Jeff A. Cowley [a], Nicholas Gudkovs [b], Peter J. Walker [a,b,*]

[a] CSIRO Livestock Industries, Queensland Bioscience Precinct, 306 Carmody Road, St. Lucia, Queensland 4067, Australia
[b] CSIRO Livestock Industries, Australian Animal Health Laboratory, 5 Portarlington Road, Geelong, Victoria 3220, Australia
[c] National Center for Genetic Engineering and Biotechnology (BIOTEC), National Science and Technology Development Agency (NSTDA), Phathumthani 12120, Thailand
[d] Center of Excellence for Shrimp Molecular Biology and Biotechnology, Faculty of Science, Mahidol University, Rama VI Road, Phyathai, Bangkok 10400, Thailand

ARTICLE INFO

Article history:
Received 1 March 2009
Returned to author for revision 15 April 2009
Accepted 20 April 2009
Available online 31 May 2009

Keywords:
Yellow head virus
Gill-associated virus
Phylogeny
Genotype
Genetic recombination

ABSTRACT

Yellow head virus (YHV) is a highly virulent pathogen of *Penaeus monodon* shrimp. It is one of six known genotypes in the yellow head complex of nidoviruses which also includes mildly pathogenic gill-associated virus (GAV, genotype 2) and four other genotypes (genotypes 3–6) that have been detected only in healthy shrimp. In this study, comparative phylogenetic analyses conducted on replicase- (ORF1b) and glycoprotein- (ORF3) gene amplicons identified 10 putative natural recombinants amongst 28 viruses representing all six genotypes from across the Indo-Pacific region. The ~4.6 kb genomic region spanning the two amplicons was sequenced for three putative recombinant viruses from Vietnam (genotype 3/5), the Philippines (genotype 5/2) and Indonesia (genotype 3/2). SimPlot analysis using these and representative parental virus sequences confirmed that each was a recombinant genotype and identified a recombination hotspot in a region just upstream of the ORF1b C-terminus. Maximum-likelihood breakpoint analysis predicted identical crossover positions in the Vietnamese and Indonesian recombinants, and a crossover position 12 nt upstream in the Philippine recombinant. Homologous genetic recombination in the same genome region was also demonstrated in recombinants generated experimentally in shrimp co-infected with YHV and GAV. The high frequency with which natural recombinants were identified indicates that genetic exchange amongst genotypes is occurring commonly in Asia and playing a significant role in expanding the genetic diversity in the yellow head complex. This is the first evidence of genetic recombination in viruses infecting crustaceans and has significant implications for the pathogenesis of infection and diagnosis of these newly emerging invertebrate pathogens.

Introduction

The yellow head complex of nidoviruses comprises yellow head virus (YHV), gill-associated virus (GAV) and at least four other closely related genotypes that occur commonly in the giant tiger shrimp (*Penaeus monodon*) in the Indo-Pacific region (Walker et al., 2001; Soowannayan et al., 2003; Wijegoonawardane et al., 2008a). YHV (designated genotype 1) was first reported as the cause of mass mortalities in shrimp ponds in Thailand in 1990 (Limsuwan, 1991) and has since been reported in other shrimp farming regions in Southeast and East Asia (Walker et al., 2001). It is a highly virulent pathogen that can cause total crop loss within several days of the first appearance of disease (Boonyaratpalin et al., 1993; Chantanachookin et al., 1993). GAV (genotype 2) was first observed as a persistent low-level infection in healthy *P. monodon* shrimp in Australia in 1994 (Spann et al., 1995). Although far less virulent than YHV, GAV causes mortalities following experimental infection of shrimp and has been associated with a slowly progressing disease called mid-crop mortality syndrome (MCMS) (Spann et al., 1997, 2003; Callinan and Jiang, 2003). The prevalence of GAV infection in healthy *P. monodon* in eastern Australia approaches 100% and it occurs commonly in healthy shrimp from Vietnam and Thailand (Walker et al., 2001; Wijegoonawardane et al., 2008a). The four other known genotypes in the yellow head complex also occur commonly in healthy *P. monodon* with a distribution that extends from Mozambique in the west through South, Southeast and East Asia (Wijegoonawardane et al., 2008a). None of these four genotypes has yet been associated with disease.

The yellow head complex viruses are enveloped, rod-shaped, (+) sense RNA viruses that are classified as a single species (*Gill-associated virus*) in the genus *Okavirus*, family *Roniviridae*, order *Nidovirales* (Walker et al., 2004). The 26,662 nt YHV genome contains four long open reading frames (ORFs). ORF1a encodes a large polyprotein

* Corresponding author. CSIRO Livestock Industries, Queensland Bioscience Precinct, 306 Carmody Road, St. Lucia, Queensland 4067, Australia. Fax: +61 3 5227 5400.
E-mail address: Peter.Walker@csiro.au (P.J. Walker).
[1] Current address: National Aquatic Resources Research and Development Agency, Crow Island, Mattakkuliya, Colombo 15, Sri Lanka.

0042-6822/$ – see front matter.
doi:10.1016/j.virol.2009.04.015

(pp1a) containing *cis*-acting papain-like protease (PLP) and 3C-like protease (3CLP) domains (Sittidilokratna et al., 2008). ORF1b overlaps ORF1a and is expressed only as a result of a (−1) ribosomal frameshift at a 'slippery' sequence upstream of a predicted pseudoknot structure in the overlap region. The extended polyprotein (pp1ab) contains 'SDD' RNA-dependent RNA polymerase, helicase, metal-ion-binding, exonuclease, uridylate-specific endoribonuclease and ribose-2′-*O*-methyl transferase domains of the replication complex (Sittidilokratna et al. 2002, 2008). ORF2 encodes the nucleoprotein (p20) which is the only polypeptide component of the helical nucleocapsid (Soowannayan et al., 2003; Sittidilokratna et al., 2006). ORF3 encodes a polyprotein (pp3) that is processed at signal peptidase type 1 cleavage sites to generate the two virion envelope glycoproteins gp116 and gp64, and an N-terminal triple-membrane-spanning fragment of unknown function (Jitrapakdee et al., 2003). The 26,235 nt GAV genome is smaller, primarily due to significant deletions in intergenic regions (IGRs), but shares ~79% overall nucleotide sequence identity with YHV (Cowley and Walker, 2002; Sittidilokratna et al., 2008). The GAV genome organisation is similar to YHV and all identified functional domains are preserved, but GAV contains an additional small open reading frame near the 3′-terminus (ORF4, 83 aa) that may be expressed at low levels in infected cells (Cowley et al., 2000; Cowley and Walker, 2002; Cowley et al., 2004a; Cowley and Walker, 2008). Like other nidoviruses, YHV and GAV transcribe a nested set of 3′-coterminal, polyadenylated, genomic and sub-genomic mRNAs (Cowley et al., 2002; Sittidilokratna et al., 2008). Partial genome sequence analysis of genotypes 3, 4 and 5 has indicated that they share a similar genome organisation and transcription strategy and are more closely related in sequence to GAV than to YHV (Wijegoonawardane et al., 2008a).

In this paper, we report evidence of natural, high frequency genetic recombination between genotypes in the YHV complex and demonstrate that recombinants can be recovered from mixed experimental infections of shrimp with YHV and GAV. Partial sequence analysis of selected recombinant genomes identified that recombination occurs preferentially at a hotspot near the C-terminus of the ORF1b coding region, suggesting modular functional separation of the structural and non-structural domains. This is the first evidence of genetic recombination in viruses infecting shrimp and has significant implications for the pathogenesis of infection and diagnosis of these newly emerging invertebrate pathogens.

Results

Phylogenetic analyses using ORF1b and ORF3 amplicons

Twenty-eight virus samples (Table 1), representing each of the six identified genotypes in the yellow head complex, were selected from a set of 57 viruses detected previously in shrimp collected from countries across the Indo-Pacific region (Wijegoonawardane et al., 2008a). Total RNA extracted from each of the samples was used as a template for RT-PCR amplification of two genomic regions. The first (668–671 nt), located in ORF1b overlapping and immediately downstream of the helicase domain, was used previously to assign genotypes (Wijegoonawardane et al., 2008a, 2008b). The second region (1287 nt in YHV) was located in the N-terminal domain of ORF3, extending from a locus 28 nt downstream of the ORF3 initiation codon, to a site beyond the internal signal peptidase cleavage site at the N-terminus of gp116. ClustalX multiple alignments of nucleotide sequences obtained from each region, and corresponding genome sequences of the YHV (EU487200) and GAV (NC010306) reference strains, were used to construct neighbour-joining phylogenetic trees (Fig. 1).

Phylogenetic analysis of the ORF1b region (Fig. 1A) identified six distinct lineages corresponding to the six genotypes identified in a similar analysis of the larger set of 57 viruses reported previously (Wijegoonawardane et al., 2008a). Genotype 1 comprised five YHV isolates collected from disease outbreak ponds in Thailand, including the Thai YHV reference strain (THA-98-Ref) isolated from Chachoengsao Province, Thailand, in 1998. Genotype 2 included the GAV reference strain (AUS-96-Ref), a second isolate from a disease

Table 1
Penaeus monodon samples selected for phylogenetic analysis in the ORF1b and ORF3 gene regions.

Sample code	Date of collection	Sample origin	Life stage	Tissues for extraction	Health status	Genotype ORF1b	Genotype ORF3
AUS-97-MCMS1	24.04.1997	Queensland, Australia	Adult	Gill	MCMS[a]	2	2
AUS-00-HL2	2000	Queensland, Australia	Adult	Lymphoid organ	Healthy	2	2
IDN-04-H4[b]	23.01.2004	Indonesia	Sub-adult	Muscle	Healthy	3	2
IDN-04-H7[b]	23.01.2004	Indonesia	Sub-adult	Muscle	Healthy	3	2
IDN-04-H10[b]	23.02.2004	Indonesia	Sub-adult	Muscle	Healthy	3	2
IND-02-H5	15.06.2002	Nellore, India	PL-14	Whole	Healthy	4	4
IND-02-H9	15.06.2002	Nellore, India	PL-15	Whole	Healthy	4	4
MOZ-04-H9	13.01.2004	Mozambique	Brooder	Gill	Healthy	6	6
MYS-03-H2[b]	06.06.2003	Malaysia	Sub-adult	Pleopod	Healthy	3	2
MYS-03-H4[b]	06.06.2003	Malaysia	Sub-adult	Pleopod	Healthy	5	2
PHL-03-H8[b]	02.10.2003	Iloilo, Philippines	PL-12	Whole	Healthy	5	3
THA-01-D10	2001	Nakorn Pathori, Thailand	Juvenile	Gill	Diseased[c]	1	1
THA-01-D8	2001	Nakorn Pathori, Thailand	Juvenile	Gill	Diseased[c]	1	1
THA-03-D29	2003	Chachoengsno, Thailand	Juvenile	Gill	Diseased[c]	1	1
THA-03-D30	2003	Chachoengsno, Thailand	Juvenile	Gill	Diseased[c]	1	1
THA-04-H20	28.03.2004	Supanburi, Thailand	PL-20	Whole	Healthy	2	2
THA-03-HA	2003	Thailand	Adult	Gill	Healthy	2	2
THA-03-HB	2003	Thailand	Adult	Gill	Healthy	2	2
THA-03-HG	2003	Thailand	Adult	Gill	Healthy	2	2
THA-03-SG21	2003	Thailand	Sub-adult	Gill	Slow growth	5	5
TWN-03-H9[b]	05.07.2003	Taiwan	Juvenile	Pleopod	Healthy	3	2
TWN-03-H11[b]	05.07.2003	Taiwan	Juvenile	Pleopod	Healthy	3	2
VNM-02-H258[b]	01.02.2002	Nha Trang, Vietnam	PL-12	Whole	Healthy	3	5
VNM-02-H278[b]	06.03.2002	Hon Chong, Vietnam	PL-12	Whole	Healthy	3	5
VNM-02-H264	03.03.2002	Ca Na, Vietnam	PL-12	Whole	Healthy	3	3
VNM-02-H93	04.02.2002	Hon Khoai, Vietnam	PL-10	Whole	Healthy	3	3
VNM-02-H6	04.02.2002	Vietnam	PL	Whole	Healthy	2	2
VNM-02-H5	01.04.2002	Vietnam	Sub-adult	Muscle	Healthy	3	3

[a] Mid-crop mortality syndrome.
[b] Recombinant genotype.
[c] Yellow head disease.

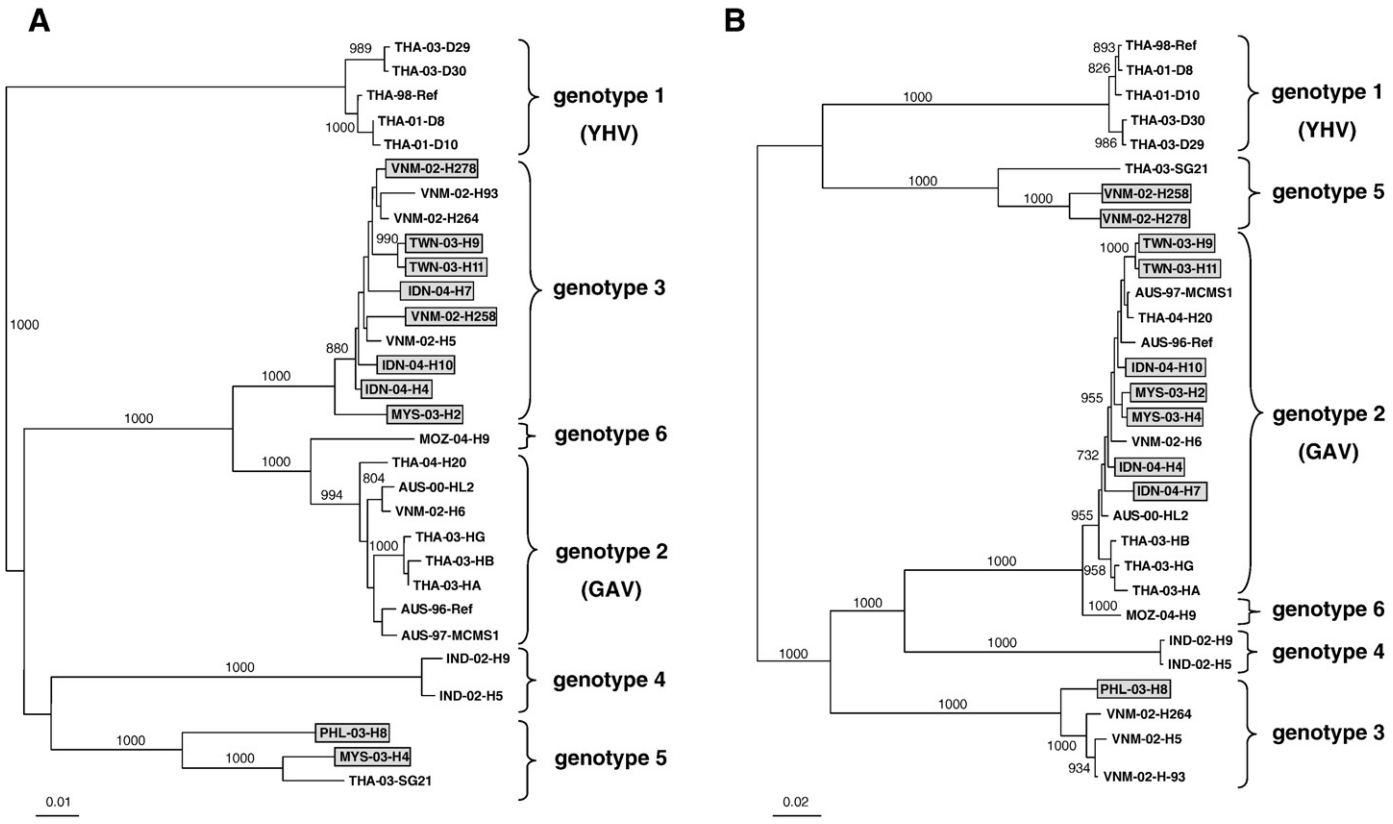

Fig. 1. Neighbour-joining phylogenetic trees constructed from a ClustalX multiple alignments of (A) a ~671 nt sequence in the ORF1b gene and (B) a ~1.25 kb sequence in the ORF3 gene amplified by RT-nested PCR from 28 yellow head complex viruses and the reference strains of YHV (THA-98-Ref) and GAV (AUS-96-Ref). The countries of origin and virus codes are described in Table 1. Bootstrap values shown at branch points indicate branching frequency in 1000 replicates. The clustering of isolates into six genetic lineages is indicated and the 10 isolates that clustered differently in the two analyses are shaded.

outbreak in Australia (AUS-97-MCMS1) and viruses detected in healthy shrimp from Australia, Thailand and Vietnam. The other four genotypes were detected only in healthy shrimp: genotype 3 included viruses detected in Vietnam, Taiwan, Indonesia and Malaysia; genotype 4 was represented by two viruses detected in India; genotype 5 comprised single viruses from the Philippines, Malaysia and Thailand that were quite divergent in sequence; genotype 6 was represented by a single virus from Mozambique.

Phylogenetic analysis of the ORF3 region also segregated the viruses into six genetic lineages (Fig. 1B). For lineages assigned as genotypes 1, 4 and 6, isolates clustered as observed using the ORF1b amplicon. However, in other lineages the isolates clustered differently. Genotype 2 included the Australian GAV reference isolate (AUS-96-Ref) and seven other viruses from Australia, Thailand and Vietnam and that clustered in ORF1b as genotype 2, as well as seven viruses that had previously clustered with viruses assigned to genotype 3 (TWN-03-H9, TWN-03-H11, IDN-04-H4, IDN-04-H7, IDN-04-H10 and MYS-03H2) or genotype 5 (MYS-03-H4). Genotype 3 comprised the remaining three Vietnamese viruses that had clustered in ORF1b as genotype 3 (VNM-02-H93, VNM-02-H264 and VNM-02-H5), and the Philippine virus (PHL-03-H8) that had previously clustered as genotype 5. Genotype 5 comprised the remaining Thai virus that had clustered in ORF1b as genotype 5 (THA-03-SG21) and two Vietnamese viruses that had previously clustered as genotype 3 (VNM-02-H258 and VNM-02-H278). In all, 10 viruses clustered differently in the phylogenies generated using the ORF1b and ORF3 amplicons, representing one-third of all viruses included in the analysis. They included viruses present in healthy shrimp collected between 2002 and 2004 from Vietnam, Taiwan, Indonesia, Malaysia and the Philippines, and represented putative recombinant viruses involving genotypes 2, 3 and 5.

Analysis of natural recombinant genotypes

For three viruses, representing putative recombinant genotypes 3/2 (IDN-04-H10), 3/5 (VNM-02-H258) and 5/3 (PHL-03-H8), the ~3.2 kb region of the genome between the ORF1b and ORF3 amplicons was amplified by RT-nested PCR using isolate-specific primers, and sequenced. The ~4.6 kb region including the terminal ORF1b and ORF3 amplicon sequences was then compared with those of viruses representing 'parental' genotypes 2 (AUS-96-Ref), 3 (VNM-02-H93) and 5 (THA-03-SG21) reported previously (Wijegoonawardane et al., 2008a). SimPlot nucleotide diversity profiles calculated for short overlapping sequences of the ~4.6 kb region confirmed that each isolate had originated through recombination (Fig. 2). The profiles revealed a reversal in sequence similarity between recombinant and parental genotypes in regions upstream and downstream of a predicted recombination site near the 3′-terminus of the ORF1b gene. In the homologous regions, the level of identity between the recombinants and genotype 2 and 3 viruses approached 100%. The level of sequence identity in homologous regions of the 'parental' genotype 5 virus and recombinants VNM-02-H258 and PHL-03-H8 was somewhat lower. This is consistent with the relatively higher sequence diversity observed amongst genotype 5 isolates compared to viruses of other genotypes (Fig. 1) (Wijegoonawardane et al., 2008a).

LARD software was used to predict recombination breakpoints in putative recombinant viruses VNM-02-H258 and IND-04-H10 and PHL-03-H8. Mean likelihood ratio (LR) values calculated from 300 simulations using jumbled parental and recombinant sequences to simulate the null hypothesis of no recombination were compared to maximum LR values obtained from analyses of the representative parental and the three recombinant isolates (Table 2). *Z*-test analysis

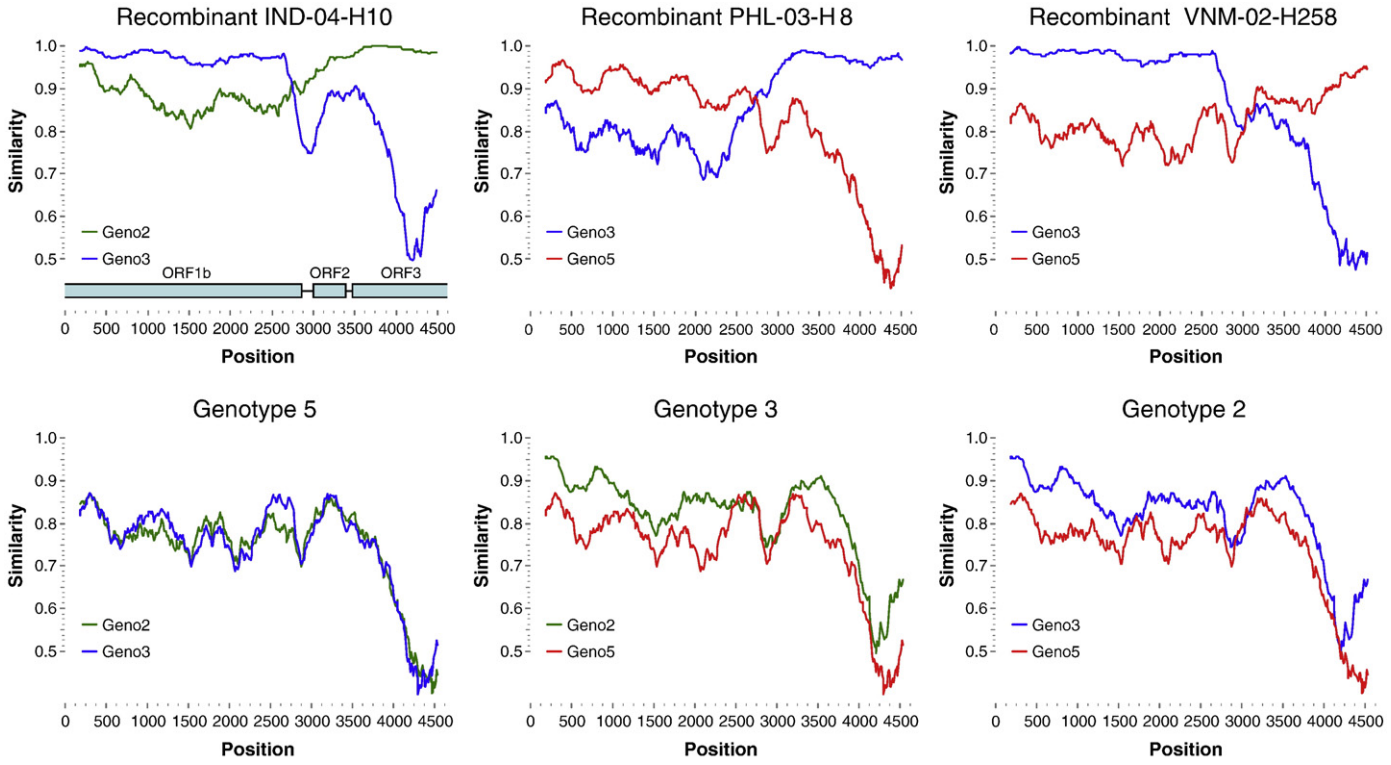

Fig. 2. SimPlot (Version 3.5.1) analysis of putative recombinants IDN-04-H10, VNM-02-H258 and PHL-03-H8 with representative parental genotypes 2, 3 and 5. Pair-wise divergence between the recombinant and each parental virus or between different genotypes over the ~4.6 kb ORF1b-ORF3 region employed a 350 nt sliding window analysed at 10 nt intervals and the default Kimura (2-parameter) Distance Model. Percentage identities at each analysis point were plotted on a line chart. The relative positions of the ORF1, ORF2 and ORF3 genes are shown in the first panel.

provided strong statistical support ($p<0.01$) for recombination in VNM-02-H258 and IND-04-H10 at the same site (GUU↓AUU) located 28 nt upstream of the ORF1b termination codon. In PHL-03-H8, the recombination breakpoint was predicted at the sequence (UAU↓AAA) located 39 nt upstream of the ORF1b stop codon. LARD also indicated significantly higher levels of nucleotide sequence identity between the putative recombinants and 'parental' genotypes in homologous regions upstream and downstream of the predicted breakpoints (Table 2). Sequence identity of the recombinants with homologous regions of the representative genotype 2 and genotype 3 viruses was in the range 96.2%–98.0%, whereas identity in the non-homologous regions reflected the divergence between genotypes (76.6%–79.3%). Sequence identity of the recombinants with homologous regions of the representative genotype 5 virus was lower (90.0%–91.4%), again reflecting the diversity amongst isolates of genotype 5 and indicating that the true parental viruses were significantly divergent in sequence from the representative genotype 5 virus (THA-03-SG21) used in this analysis.

Exclusion of 'polymerase-jumping' artefacts

An experiment was conducted to exclude the possibility that the putative recombinant genomes were generated as an artefact of 'polymerase-jumping' during RT-PCR amplification from shrimp carrying mixed infections with two genotypes. Consensus degenerate PCR primers targeted to regions conserved amongst putative recombinants IDN-04-H10 and VNM-02-258, and representative parental genotype 2 (AUS-00-H11), genotype 3 (VNM-02-H93) and genotype 5 (THA-03-SG21) viruses, were used to amplify a ~1.5 kb region spanning the recombination hotspot at the end of ORF1b.

Table 2
Nucleotide sequence identities between recombinant isolates and parental genotypes in regions upstream and downstream of the recombination site and recombination likelihood values generated using LARD software.

Recombinants	Sequence identity upstream (%)[a]	Sequence identity downstream (%)[b]	Mean LR no recombination[c]	Max LR recombination	*Z*-test value (*p*)
IDN-03-H10			5.3 ± 1.7	319.1	<0.01
H10: Genotype 3	97.7	79.1			
H10: Genotype 2	89.1	97.5			
Genotype 3:Genotype 2	88.2	79.3			
VNM-02-H258			5.6 ± 1.7	271.5	<0.01
H258: Genotype 3	98.0	74.3			
H258: Genotype 5	82.5	90.0			
Genotype 3:Genotype 5	82.1	76.7			
PHL-03-H8			5.6 ± 1.7	361.0	<0.01
H8: Genotype 5	91.4	75.6			
H8: Genotype 3	81.9	96.2			
Genotype 5:Genotype 3	82.1	76.6			

[a] Gap-less pairwise comparisons of nucleotide sequence upstream of the breakpoint.
[b] Gap-less pairwise comparisons of the nucleotide sequence downstream of the breakpoint.
[c] 300× simulations.

Table 3
PCR primer pair combinations and genotype specificity for confirmation of natural recombinant genotypes IDN-04-H10 and VNM-02-H258.

Primer pair[a]	Primer sequence specificity	Amplicon	
IDN-04-H10			
P11	Geno3-Recom10F	Genotype 3 + IDN-04-H10	1196 bp
	Geno3-Sp-R	Genotype 3	
P12	Geno2-Sp-F	Genotype 2	
	Geno2-Recom10R	Genotype 2 + IDN-04-H10	
P13	Geno2-Sp-F	Genotype 2	
	Geno3-Sp-R	Genotype 3	
P14	Geno3-Recom10F	Genotype 3 + IDN-04-H10	
	Geno2-Recom10R	Genotype 2 + IDN-04-H10	
VNM-02-H258			
P21	Geno3-Recom258F	Genotype 3 + VNM-02-H258	996 bp
	Geno3-Sp-2R	Genotype 3	
P22	Geno5-Sp-F	Genotype 5	
	Geno5-Recom258R	Genotype 5 + VNM-02-H258	
P23	Geno5-Sp-F	Genotype 5	
	Geno3-Sp-2R	Genotype 3	
P24	Geno3-Recom258F	Genotype 3 + VNM-02-H258	
	Geno5-Recom258R	Genotype 5 + VNM-02-H258	

[a] Primer codes: genotype (Geno), recombinant (Recom), forward primer (F), reverse primer (R).

Nested primers with specificity for genotype 2, genotype 3 or genotype 5 sequences were then used to amplify internal regions of ~1.2 kb (genotypes 2 and 3) or ~1.0 kb (genotypes 3 and 5). The primer pair combinations and their genotype specificities are shown in Table 3. PCR data are shown in Fig. 3. Nested PCR employing a genotype 3 forward primer and genotype 2 reverse primer amplified the expected ~1.2 kb product only for recombinant IDN-04-H10, and not the 1:1 mixture of genotypes 2 and 3 (Fig. 3A). Similarly, nested PCR employing a genotype 3 forward primer and a genotype 5 reverse primer amplified the expected ~1.0 kb product only for recombinant VNM-02-H258, and not the 1:1 mixture of genotypes 3 and 5 (Fig. 3B). The data confirm that the sequences flanking the predicted breakpoints were derived from recombinant genotypes.

Recovery of recombinant viruses from experimental infections in shrimp

P. monodon shrimp were infected simultaneously with YHV (stock inoculum diluted 10^{-5} or 10^{-6}) and GAV (stock inoculum diluted 10^{-1}). The dose for each virus was selected to ensure mortalities occurred within 5–10 days of infection and reflected the much higher virulence of YHV. Moribund shrimp were sampled at day 9 post-infection from each mixed-infection group and from control groups infected with YHV or GAV only. Total RNA was extracted from lymphoid organs and used as a template for RT-PCR amplification of a genomic region spanning the recombination breakpoints identified in the natural recombinants. Due to a large sequence deletion in the ORF1b-ORF2 IGR of GAV and the relative positions of PCR primers, the region targeted for amplification comprised 419 nt in GAV and 686 nt in YHV. As shown in Fig. 4, RT-PCR using primers with specificity for YHV in ORF1b (YHV-ORF1b-2f) and GAV in ORF2 (GAV-ORF2-2r) amplified products from the two co-infected shrimp (AL9 and BL4) tested. Direct sequence analysis showed that the ~420 bp product (band 1) obtained from each shrimp was derived from a YHV/GAV recombinant genome (Figs. S2A and S2B). In each, the recombination breakpoint was located at a similar site within a 25 nt segment near to the C-terminus of ORF1b. Multiple products were amplified from shrimp

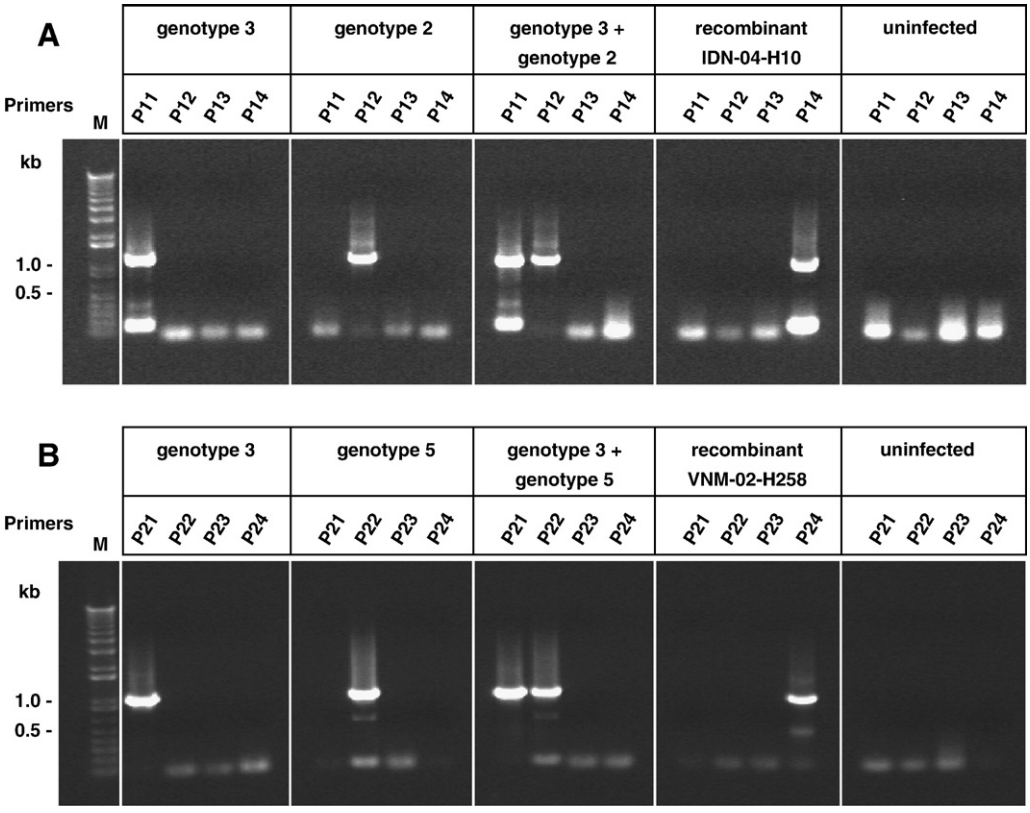

Fig. 3. Differential RT-nested PCR amplification of the genome region spanning ORF1b-ORF2 and encompassing the recombination hotspot identified in recombinants IDN-04-H10 and VNM-02-H258. RNA of these recombinants as well as 1:1 RNA mixtures to representative genotype 2 and 3 viruses (AUS-00-HL11:VNM-02-H93) and genotype 3 and 5 viruses (VNM-02-H93:THA-03-SG21) and RNA of each genotype 2, 3 and 5 virus and an uninfected shrimp were amplified by RT-PCR using the consensus PCR primer pair Con-2F:Con-2R (Table S1). Differential nested PCR amplification of these PCRs was then undertaken using either (A) primer permutations P11, P12, P13 and P14 specific to genotypes 2 and 3 or (B) primer permutations P21, P22, P23 and P24 specific to genotypes 3 and 5 (Tables S1 and S2). Amplified DNA was resolved in a 1% agarose-TAE gel. M = 1 kbp PLUS DNA Ladder (Invitrogen).

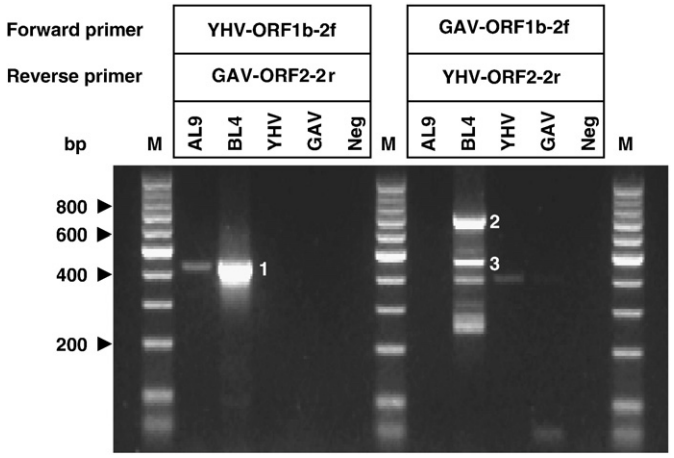

Fig. 4. Differential RT-PCR amplification of a genome region spanning the C-terminus of ORF1b to the N-terminus of ORF2 using RNA isolated from shrimp infected with YHV or GAV alone or co-infected with YHV and GAV (samples AL9 and BL4). PCR utilised the YHV-specific and GAV-specific primer combinations YHV-ORF1b-2f:GAV-ORF2-2r and GAV-ORF1b-2f:YHV-ORF2-2r (Table S1). Amplified DNA was resolved in a 2% agarose-TAE gel. M = BenchTop 100 bp DNA Ladder (Promega). DNA products labelled 1, 2 and 3 obtained with co-infection samples AL9 and BL4 were sequenced.

BL4 in the RT-PCR using primers with specificity for GAV in ORF1b (GAV-ORF1b-2f) and YHV in ORF2 (YHV-ORF2-2r) (Fig. 4). Sequence analysis of the ~700 bp and ~480 bp products (BL4-2 and BL4-3) indicated that they were derived from recombinant genomes with a GAV/YHV orientation (Figs. S2C and S2D). In product BL4-2, the recombination breakpoint was located in the same ORF1b region as identified in the YHV/GAV recombinants and sequence ambiguities at multiple sites indicated the likely presence of several similar recombinant genomes with similar but distinct breakpoints. In product BL4-3, the breakpoint occurred within a 16 nt region of a highly conserved domain that contains the transcription regulatory sequence (TRS) and the 5′-end of the ORF2 mRNA (Cowley et al., 2002), and its location beyond the YHV sequence insertion accounted for the smaller amplicon size. The data indicate that recombination can occur readily in shrimp co-infected with YHV and GAV, involve different sites, and generate recombinants in either orientation.

Discussion

Based on phylogenetic analyses of sequences amplified from a relatively conserved region of the ORF1b gene, we have recently identified at least six distinct genotypes in the yellow head complex of nidoviruses (Wijegoonawardane et al., 2008a). YHV (genotype 1) was detected only in shrimp from Thailand and Taiwan with typical signs of yellow head disease. GAV (genotype 2) occurs commonly in healthy *P. monodon* in Australia and parts of Southeast Asia, and it has been associated with a condition called mid-crop mortality syndrome. The four other genotypes were detected in healthy *P. monodon* from Mozambique, India, Thailand, Malaysia, Indonesia, Vietnam, the Philippines and Taiwan. In this paper, we report evidence of homologous genetic recombination involving four of the six genotypes (genotypes 1, 2, 3 and 5). Natural recombinants derived from genotypes 2, 3 and 5 were detected by their differential clustering in phylogenetic analyses of sequences amplified from two distant regions of the genome, and this was confirmed for several of these viruses by sequencing and SimPlot analysis of the ~4.6 kb genomic region encompassing the two amplicons. Genetic recombination was also demonstrated experimentally in shrimp co-infected with two of the genotypes (YHV and GAV) that have been associated with disease outbreaks in farmed shrimp in Thailand and Australia. This is the first evidence of homologous genetic recombination in viruses infecting crustaceans.

Homologous and non-homologous genetic recombination has been reported to occur naturally and experimentally in coronaviruses (Lai et al., 1985; Kusters et al. 1990; Wang et al., 1993; Herrewegh et al., 1995; Woo et al., 2006), toroviruses (Smits et al., 2003) and arteriviruses (Li et al., 1999; Yuen et al., 1999; Molenkamp et al., 2000). In experimental co-infections, recombination between coronavirus strains can occur at a frequency as high as 25% (Baric et al., 1990). Natural recombination in nidoviruses also appears to occur commonly and to have resulted in gene rearrangements and the generation of chimeric viruses with ancestors of vastly different lineages (Luytjes et al., 1988; Snijder et al., 1991; Motokawa et al., 1995). The data reported here indicate that homologous genetic recombination between yellow head complex viruses of the *Roniviridae* can also occur readily, both in experimental co-infections and naturally. In this study, 10 of 30 viruses were identified as recombinant genotypes by comparative phylogenetic analysis. Although the frequency with which recombinants were generated experimentally has not yet been assessed, the identification of multiple recombinant genotypes of different conformation in individual moribund shrimp following co-infection with YHV and GAV indicates that recombination occurs readily and that at least some recombinant genomes survive multiple rounds of replication.

The creation and survival of a viable recombinant virus are subject to many molecular and biological constrains (Worobey and Holmes, 1999). There must be opportunity for co-infection of the host and simultaneous infection of an individual host cell, replication must occur at the same intracellular location, template switching must occur and generate a viable genome, and any viable recombinant virus must be suitably fit to survive competition from both parental and other recombinant viruses. The high frequency at which natural recombinant genotypes were detected in this study indicates that these requirements are readily met by roniviruses and this may reflect the frequency with which mixed infections occur in shrimp. Yellow head complex viruses occur very commonly in healthy *P. monodon* shrimp throughout their natural distribution range across the Indo-Pacific (Wijegoonawardane et al., 2008a). The prevalence of GAV infection in healthy *P. monodon* postlarvae, juveniles and broodstock sourced from the wild and from shrimp hatcheries and farms along the east coast of Australia between 1998 and 2001 was observed to approach 100% (Walker et al., 2001). A survey conducted in 2000 identified genotype 3 in 25 of 38 healthy *P. monodon* broodstock collected from hatcheries in central Thailand and a survey of ~200 *P. monodon* sampled from across the Indo-Pacific region between 1997 and 2004 detected evidence of ronivirus infection in >25% of the shrimp (Wijegoonawardane et al., 2008a). Although there has been no systematic study of the prevalence of natural co-infection with ronivirus genotypes, co-infection with multiple shrimp viruses appears to occur commonly (Manivannan et al., 2002; Chayaburakul et al., 2004; Flegel et al., 2004; Hoa et al., 2005; Natividad et al., 2006). This is likely a consequence of life-long persistent infections, the efficiency of both vertical and horizontal transmission, the lack of adaptive immunity in shrimp, and husbandry practices which commonly mix the progeny of multiple broodstock to seed aquaculture ponds (Walker et al., 2001; Johnson et al., 2008; Walker and Mohan, 2009).

This study detected a high prevalence of naturally-occurring recombinants, but they were detected exclusively in shrimp collected from Southeast and East Asia and were derived only from genotypes 2, 3 and 5. This most likely reflects the bias of sample numbers from this region where these three genotypes are most prevalent (Wijegoonawardane et al., 2008a). However, it may also indicate that the natural course of virus-host co-evolution has been disrupted by the vast international trade in live shrimp. In Australia, where the importation of live crustaceans is prohibited, GAV is endemic and occurs at very high prevalence in *P. monodon*. No other genotype has been detected in Australia despite the analysis of very large numbers of shrimp

samples since 1996 and GAV has not been detected in natural populations of other penaeid shrimp species which are susceptible to experimental infection (Spann et al., 2000; Walker et al., 2001). Analysis of the limited numbers of samples sourced from India and Mozambique also suggests geographic isolation of genotypes 4 and 6 in regions where importation of live shrimp for aquaculture is rare (Wijegoonawardane et al., 2008a). This suggests that *P. monodon* is the natural host of GAV and possibly other genotypes and that there has been long-term co-evolution of the genotypes in this species. However, contrary to the situation in Australia, India and Mozambique, there has been a prolific trade in live *P. monodon* amongst countries in Southeast and East Asia, including the importation of stock from Australia and elsewhere. This appears to have provided adequate opportunity for new genotypes to be introduced and mixed with genotypes endemic to the region.

Although YHV/GAV recombinant viruses were readily generated in experimental co-infections, no evidence of natural recombination involving YHV was found. There are reports that YHV (genotype 1) can occur as a persistent infection in healthy shrimp (Pasharawipas et al., 1997; Natividad et al., 2002; de la Rosa-Velez et al., 2006). However, in the only published prevalence study in which genotypes have been determined (Wijegoonawardane et al., 2008a), genotype 1 was detected only in *P. monodon* from yellow head disease outbreaks in Thailand and Taiwan. There is no evidence that any other genotype can cause yellow head disease and, although GAV can cause mortalities, the LD_{50} of YHV ($10^{-11.5}$) determined in bioassays is 10^6 to 10^8-fold lower than GAV (Sittidilokratna et al., 2009). This suggests that YHV may have undergone a recent genetic change that has substantially elevated its virulence for *P. monodon* or that it may be naturally endemic in another, more resistant, penaeid or metapenaeid shrimp species. If the latter, the opportunity for co-infection involving YHV and another genotype could be relatively rare. Nevertheless, the widespread prevalence of infection with other genotypes and the capability for YHV to recombine experimentally with GAV indicate that the generation of natural YHV recombinants may be inevitable and have significant consequences for the spread of virulent genotypes and disease in penaeid shrimp.

Sequence analysis of three of 10 natural recombinant viruses identified a likely recombination hotspot just upstream of the C-terminus of the ORF1b coding region. Recombination hotspots have been identified in many animal and plant viruses, including coronaviruses (Makino et al., 1986; Banner et al., 1990; Jia et al., 1995; Lee and Jackwood, 2000; van Vugt et al., 2001), bromoviruses (Nagy et al., 1999) geminiviruses (Monci et al., 2002) and luteoviruses (Moonan et al., 2000). Although specific sequence elements, such as stretches of AU-rich sequence, may enhance recombination frequency (Shapka and Nagy, 2004), a study of mouse hepatitis coronavirus has shown that recombination events are generally random and that hotspots arise as a result of subsequent selective pressure on the pool of recombinant genomes rather than elevated site-specific recombination rates (Banner and Lai, 1991). Analysis of YHV/GAV recombinants generated experimentally under conditions in which the selective pressure was relatively limited identified recombination breakpoints in a similar genomic region to the hotspot identified in natural recombinants (the ORF1b C-terminus and the downstream IGR). However, as PCR primers used to detect the experimentally-generated recombinants were intentionally targeted to this region, the possibility that recombination has occurred with similar frequency in other regions of the genome has not yet been exhaustively explored. The location of the identified hotspot in the natural recombinants is near the junction between the 5′-terminal ORF1a and ORF1b genes encoding non-structural replicase proteins and downstream ORF2 and ORF3 genes encoding the virion structural proteins. Natural selection of such recombinants may be driven by a need to maintain efficient interactions amongst these functionally distinct sets of proteins.

The finding that natural recombinants occur commonly in *P. monodon* shrimp in Asia presents significant practical issues for genotype assignment and for the detection and management of viruses that may present significant disease risks. As yellow head complex nidoviruses occur at high prevalence in healthy wild and cultured shrimp, methods that specifically detect pathogenic types are essential for farm-level diagnosis and the containment of transboundary disease spread. These methods are currently based on detection of YHV and GAV and their discrimination from other 'non-pathogenic' genotypes (Wongteerasupaya et al., 1997; Cowley et al., 2004b; Wijegoonawardane et al., 2008b). However, observations presented here that genotype 2 (GAV) and genotype 3 have recombined naturally with each other and with genotype 5, and that YHV also has the potential for natural recombination, underline a need for further research to better understand the molecular basis of pathogenesis in roniviruses.

Materials and methods

Origin of viruses and shrimp samples

The *P. monodon* shrimp samples used in this study were selected from a set of 57 collected between 1997 and 2004 from various sites across the Indo-Pacific region. Samples comprised pools of postlarvae, or gill tissue, pleopods or whole heads of juvenile to adult shrimp (Wijegoonawardane et al., 2008a). Sample details and virus designations are listed in Table 1. Experimental infections used the Chachoengsao/1998 reference strain of YHV (THA-98-Ref) and the Queensland/1996 reference strain of GAV (AUS-96-Ref), the origins of which have been described previously (Spann et al., 1997; Sittidilokratna et al., 2002).

Experimental co-infections

Experimental infections were conducted in ~20 g *P. monodon* shrimp obtained from a single pond at a commercial farm in Pathumthani, Thailand. The shrimp were maintained at ambient temperature (25 °C–28 °C) in artificial sea water and acclimated for several days prior to experimental use as described previously (Sittidilokratna et al., 2009). To confirm the absence of pre-existing YHV or GAV infection, the batch of shrimp was screened using a commercial nested RT-PCR test kit (IQ2000, Farming Intelligene Technology Corp., Taiwan) (Cowley et al., 2004b). Filtered stock inoculums of YHV and GAV reference strains were prepared as described previously from the homogenised cephalothoraxes of infected shrimp (Spann et al., 1997; Sittidilokratna et al., 2002). Each stock inoculum was titrated prior to use by inoculating groups of 10 shrimp in individual tanks with 100 µl per shrimp of 10-fold dilutions of the stock inoculum in lobster hemolymph medium (LHM).

Co-infections were conducted under the same experimental conditions in groups of 10 shrimp by injection with (A) GAV diluted 10^{-1} and YHV diluted 10^{-5} or (B) GAV diluted GAV 10^{-1} and YHV diluted 10^{-6}. Groups were also injected with YHV and GAV alone or with LHM. At 9–10 days post-injection, infected shrimp became moribund and were sampled. Lymphoid organ tissue was collected directly into TRIzol® Reagent (Invitrogen) and stored at −80 °C until used for RNA extraction.

RNA extraction and cDNA synthesis

Total RNA was extracted from pools of 10–15 postlarvae or from approximately 10–50 mg shrimp tissue using TRIzol™ Reagent, quantified and stored at −80 °C as described previously (Wijegoonawardane et al., 2008a). cDNA was synthesized using 1.0–3.0 µg RNA in a 20 µl reaction containing 50 ng random hexamer primers (Promega), 1 mM each dNTP and 100 U Superscript III reverse

transcriptase (Invitrogen) as described in the manufacturer's protocol, and stored at −20 °C.

PCR amplification and sequence analysis

The ORF1b amplicon

RT-PCR amplification and sequence analysis of a segment of the ORF1b gene amplicon have been described previously (Wijegoonawardane et al., 2008a). The sequences of this 668–671 nt amplicon for a set of 57 viruses, including the 28 used in this study, have been deposited in GenBank under accession numbers EU784980–EU785041.

The ORF3 amplicon

Degenerate PCR primers (ORF3-1F-P and ORF3-5R-P) were designed to amplify a region extending from the IGR upstream of ORF3 to a locus in ORF3 beyond the signal peptidase cleavage site at the gp116 N-terminus (Cowley and Walker, 2002; Jitrapakdee et al., 2003). Primer degeneracy accommodated sequence differences amongst isolates of YHV (genotype 1), GAV (genotype 2) and genotypes 3 and 4. Degenerate nested PCR primers (ORF3-2F-N and ORF3-4R-N) designed to target more conserved sequences were used to amplify a 1322 nt sequence corresponding to nucleotides 20,991–22,312 in the YHV genome (GenBank EU487200). The regions targeted by the PCR and nested PCR primers are shown in Fig. S1. Primer sequences are listed in Table S1.

In the PCR, 2 μl random-primed cDNA (equivalent to 100–300 ng total RNA) was amplified in a 25 μl reaction containing 1× *Taq* polymerase buffer (10 mM Tris–HCl pH 9.0, 50 mM KCl, 0.1% Triton X-100), 3.0 mM 25 mM $MgCl_2$, 17.5 pmoles of each primer, 200 μM μl of each dNTP and 1.4 U *Taq* DNA polymerase (Fisher Biotech, Australia). DNA was amplified in an *i*Cycler (Bio-Rad) using the cycling conditions 94 °C/1 min, 35 cycles of 94 °C/30 s, 56 °C/30 s and 72 °C/90 s, and then 72 °C/7 min. A 2 μl aliquot of the PCR was amplified in the nested PCR (25 μl) prepared as above except for the use of the nested primers. Thermal cycling conditions were the same except that the extension time was 75 s. DNA was resolved in 0.8% agarose-TAE gels containing 0.5 μg/ml ethidium bromide to confirm the expected ~1300 bp product had been amplified, purified using a QIAquick PCR purification column (QIAGEN) and quantified. Cycle sequencing used 20–50 ng DNA, ABI Prism BigDye Terminator V3.1 reagent (Applied Biosystems Inc.) and 3.3 pmol of the nested PCR primers. To obtain complete sequence coverage in both orientations, additional sequences were generated using internal degenerate primers ORF3-SF9 and ORF3-SR3 designed to accommodate sequence variations amongst genotypes 1, 2, 3 and 4. Isolate-specific primers ORF3-SF10 and ORF3-SF11 were used to obtain complete sequences of isolates VNM-02-H258, VNM-02-H278 and THA-03-D30. Primer sequences are listed in Table S1. Sequence data was generated at the Australian Genome Research Facility, Brisbane, Australia and chromatograms were edited using SeqEd 1.0.3 (ABI). The sequences have been deposited in GenBank under accession numbers FJ428584–FJ428613.

The region between the ORF1b and ORF3 amplicons

The ~3.2 kb region between the ORF1b and ORF3 amplicons was amplified for putative recombinants IDN-04-H10, VNM-02-H258 and PHL-03-H8, and representative isolates of genotype 3 (VNM-02-H93) and genotype 5 (THA-03-SG21). PCR and nested PCR utilised sequence-specific primers designed to the ORF1b and ORF3 gene sequences of each virus (Table S1) and the Expand Long Distance PCR system (Roche Applied Science). In the PCR, 2 μl random-primed cDNA was amplified in a 50 μl reaction containing Expand buffer 3, 3 mM $MgCl_2$, 500 μM each dNTP (Fisher Biotech), 35 pmol of each primer and 3.75 U Expand enzyme mix. The thermal cycling conditions were 94 °C/1 min, 10 cycles of 94 °C/25 s, 60 °C/30 s, 68 °C/45–155 s (dependent on the amplicon length), plus 30 additional cycles in which the extension time was increased sequentially by 7 s per cycle, and a final extension step of 68 °C/7 min. For isolate PHL-03-H8, the PCR annealing temperature was lowered to 53 °C. In the nested PCRs, 2 μl of the PCR was amplified using the same conditions. DNA products were purified using QIAquick PCR purification columns and sequenced in both orientations as described above using primers listed in Table S1. For genotype 5 isolate THA-03-SG21, the sequence of the same ~3.2 kb region was obtained from a plasmid containing an cDNA insert amplified using primers Geno5-F1-P and Geno5-R2-N (Table S1) and the Superscript II One-Step RT-PCR system (Invitrogen) as described previously (Wijegoonawardane et al., 2008a). The sequences have been deposited in GenBank under accession numbers FJ438530–FJ438532.

The region spanning the recombination breakpoints

To exclude the possibility of polymerase-jumping artefacts during PCR, an RT-nested PCR designed to amplify a ~1.0–1.2 kb region spanning the predicted recombination breakpoints was applied to putative recombinant viruses and mixtures of viruses representing the putative parental genotypes. In the PCR, random-primed cDNA was amplified using consensus degenerate primers (Con-2F and Con-2R) targeted to sequences relatively conserved in the ORF1b and ORF3 genes (Table S1). PCR was conducted in a 25 μl reaction containing 2 μl random-primed cDNA (equivalent to 100 ng total RNA), 1× *Taq* polymerase buffer (10 mM Tris–HCl pH 9.0, 50 mM KCl, 0.1% Triton X-100), 3 mM $MgCl_2$, 17.5 pmol of each consensus primer, 200 μM each dNTP and 1.4 U *Taq* DNA polymerase, using the cycling conditions 94 °C/60 s followed by 35 cycles of 94 °C/30 s, 53 °C/30 s, 72 °C/90 s. The second step employed nested PCR primer pair combinations P11, P12, P13 and P14 or combinations P21, P22, P23 and P24 (Table 3). A 1 μl aliquot of the PCR was amplified in nested PCRs (25 μl) containing each primer pair combination and using the same cycling conditions except that the annealing temperature was raised to 62 °C and the extension time reduced to 75 s. To detect recombinants in shrimp co-infected experimentally with YHV and GAV, sequence-specific PCR primers (Table S1) were designed to non-conserved sequences in the ORF1b gene (YHV-ORF1b-2f and GAV-ORF1b-2f) and surrounding the initiation codon of ORF2 (YHV-ORF2-2r and GAV-ORF2-2r). Random-primed cDNA was amplified in a 25 μl reaction containing QIAGEN HotStarTaq Master Mix and 20 μM reciprocal PCR primer pairs using the cycling conditions 95 °C/15 min, 40 cycles of 94 °C/30 s, 58 °C/30 s and 72 °C/60 s, and then 72 °C/7 min. DNA products were purified using QIAquick PCR purification columns and sequenced in both orientations as above using the PCR primers.

Sequence alignments and phylogenetic analyses

ClustalX (1.82) (Thompson et al., 1994) was used to generate pairwise and multiple alignments of nucleotide sequences which were displayed using Genedoc 5.2 (http://www.psc.edu/biomed/gendoc). Phylogenetic relationships were deduced from ClustalX data files using the neighbour-joining distance algorithm. Bootstrapping of tree nodes employed 1000 replicates.

Similarity and breakpoint analyses

SimPlot V3.5.1 (Lole et al., 1999) was used to identify likely recombination sites. ClustalX alignments of the ~4.6 kb genome sequence spanning the ORF1b and ORF3 amplicons were generated using each of the three putative recombinant viruses and representative parental genotypes. Pair-wise divergence values plotted in SimPlot line charts employed a sliding window of 350 nt calculated at 10 nt intervals.

Recombination crossover positions or 'breakpoints' were predicted from ClustalX multiple sequence alignments using the LARD software (Holmes et al., 1999) which calculates a mean likelihood ratio (LR)

from 300 simulations using jumbled parental and recombinant sequences to simulate the null hypothesis (no recombination). A maximum LR value is determined from the values calculated by random division of the aligned sequences into two regions to determine which possess the longest tree branch lengths between the recombinant and each parent. The breakpoint nucleotide is predicted to that flanked by sequences possessing the highest maximum LR. To assess whether the recombination model provides a significantly better fit to the data set than the null hypothesis, a *Z* test is used to analyse the maximum LR values against a null distribution of LR values generated using the Monte Carlo simulation of randomised sequences. Sequences were simulated 300 times using the maximum-likelihood model parameters and sequence lengths from the real data using Seq-Gen (Rambaut and Grassly, 1997). Simulated sequences were then subjected to the same breakpoint analysis as the real data to produce the distribution of likelihood ratios expected if no recombination had occurred among them.

Acknowledgments

The authors wish to thank Ms Linda Nielsen and Ms Wansika Kiatpathomchai for supplying shrimp samples and Prof. Tim Flegel for permitting access to facilities at CENTEX Shrimp, Mahidol University, Bangkok, Thailand. This research and the PhD undertaken by PKMW were funded, in part, by the Asian Development Bank via the National Aquatic Resources Research and Development Agency of Sri Lanka, and by the Food and Agricultural Organisation (FAO) of the United Nations.

Appendix A. Supplementary data

Supplementary data associated with this article can be found, in the online version, at doi:10.1016/j.virol.2009.04.015.

Note-added-in-proof

Since this paper was submitted, evidence of probable recombinant yellow head complex virus has been reported by Gangnonngiw et al. (2008) Virology 385, 161–168.

References

Banner, L.R., Lai, M.M., 1991. Random nature of coronavirus RNA recombination in the absence of selection pressure. Virology 185, 441–445.

Banner, L.R., Keck, J.G., Lai, M.M., 1990. A clustering of RNA recombination sites adjacent to a hypervariable region of the peplomer gene of murine coronavirus. Virology 175, 548–555.

Baric, R.S., Fu, K., Schaad, M.C., Stohlman, S.A., 1990. Establishing a genetic-recombination map for murine coronavirus strain A59 complementation groups. Virology 177, 646–656.

Boonyaratpalin, S., Supamattaya, K., Kasornchandra, J., Direkbusaracom, S., Aekpanithanpong, U., Chantanachookin, C., 1993. Non-occluded baculo-like virus, the causative agent of yellow head disease in the black tiger shrimp (*Penaeus monodon*). Fish Path. 28, 103–109.

Callinan, R.B., Jiang, L., 2003. Fatal virus-associated peripheral neuropathy and retinopathy in farmed *Penaeus monodon* in eastern Australia. II. Outbreak descriptions. Dis. Aquat. Org. 53, 195–202.

Chantanachookin, C., Boonyaratpalin, S., Kasornchandra, J., Direkbusarakom, S., Ekpanithanpong, U., Supamataya, K., Sriurairatana, S., Flegel, T.W., 1993. Histology and ultrastructure reveal a new granulosis-like virus in *Penaeus monodon* affected by yellow-head disease. Dis. Aquat. Org. 17, 145–157.

Chayaburakul, K., Nash, G., Pratanpipat, P., Sriurairatana, S., Withyachumnarnkul, B., 2004. Multiple pathogens found in growth-retarded black tiger shrimp *Penaeus monodon* cultivated in Thailand. Dis. Aquat. Org. 60, 89–96.

Cowley, J.A., Walker, P.J., 2002. The complete sequence of gill-associated virus of *Penaeus monodon* prawns indicates a gene organisation unique amongst nidoviruses. Arch. Virol. 147, 1977–1987.

Cowley, J.A., Walker, P.J., 2008. Molecular biology and pathogenesis of roniviruses. In: Perlman, S., Gallagher, T., Snijder, E.J. (Eds.), Nidoviruses. ASM Press, Washington D.C., pp. 361–377.

Cowley, J.A., Dimmock, C.M., Spann, K.M., Walker, P.J., 2000. Gill-associated virus *Penaeus monodon* prawns: an invertebrate nidovirus with ORF1a and ORF1b gene related arteri- and coronaviruses. J. Gen. Virol. 81, 1473–1484.

Cowley, J.A., Dimmock, C.M., Walker, P.J., 2002. Gill-associated nidovirus of *Penaeus monodon* prawns transcribes 3′-coterminal subgenomic RNAs that do not possess 5′-leader sequences. J. Gen. Virol. 83, 927–935.

Cowley, J.A., Cadogan, L.C., Spann, K.M., Sittidilokratna, N., Walker, P.J., 2004a. The gene encoding the nucleocapsid protein of gill-associated nidovirus of *Penaeus monodon* prawns is located upstream of the glycoprotein gene. J. Virol. 78, 8935–8941.

Cowley, J.A., Cadogan, L.C., Wongteerasupaya, C., Hodgson, R.A.J., Spann, K.M., Boonsaeng, V., Walker, P.J., 2004b. Multiplex RT-nested PCR differentiation detection of gill-associated virus (Australia) and yellow head virus (Thailand) of *Penaeus monodon*. J. Virol. Meth. 117, 49–59.

de la Rosa-Velez, J., Cedano-Thomas, Y., Cid-Becerra, J., Mendez-Payan, J.C., Vega-Perez, C., Zambrano-Garcia, J., Bonami, J.R., 2006. Presumptive detection of yellow head virus by reverse transcriptase-polymerase chain reaction and dot-blot hybridization in *Litopenaeus vannamei* and *L. stylirostris* culture on the northwest coast of Mexico. J. Fish Dis. 29, 717–726.

Flegel, T.W., Nielsen, L., Thamavit, V., Kongtim, S., Pasharawipas, T., 2004. Presence of multiple viruses in non-diseased cultivated shrimp at harvest. Aquaculture 240, 55–68.

Herrewegh, A.A.P.M., Vennema, H., Horzinek, M.C., Rottier, P.J.M., de Groot, R.J., 1995. The molecular genetics of feline coronaviruses: comparative sequence analysis of the ORF7a/7b transcription unit of different biotypes. Virology 212, 622–631.

Hoa, T.T.H., Hodgson, R.A.J., Oanh, D.T.H., Phuong, N.T., Preston, N.J., Walker, P.J., 2005. Genotypic variations in tandem repeat DNA segments between ribonucleotide reductase subunit genes of white spot syndrome virus (WSSV) isolates from Vietnam. In: Reantaso, M.B., Lester, R.G., Walker, P.J. (Eds.), Diseases in Asian Aquaculture V. Fish Health Section. Asian Fisheries Society, Manila, pp. 339–351.

Holmes, E.C., Worobey, M., Rambaut, A., 1999. Phylogenetic evidence for recombination in dengue viruses. Mol. Biol. Evol. 16, 405–409.

Jia, W., Karaca, K., Parrish, C.R., Naqi, S.A., 1995. A novel variant of avian infectious bronchitis virus resulting from recombination among three different strains. Arch. Virol. 140, 259–271.

Jitrapakdee, S., Unajak, S., Sittidilokratna, N., Hodgson, R.A., Cowley, J.A., Walker, P.J., Panyim, S., Boonsaeng, V., 2003. Identification and analysis of gp116 and gp64 structural glycoproteins of yellow head nidovirus of *Penaeus monodon* shrimp. J. Gen. Virol. 84, 863–873.

Johnson, K., van Hulten, M.C.W., Barnes, A.C., 2008. "Vaccination" of shrimp against viral pathogens: phenomenology and underlying mechanisms. Vaccine 26, 4885–4892.

Kusters, J.G., Jager, E.J., Niesters, H.G., van der Zeijst, B.A., 1990. Sequence evidence for RNA recombination in field isolates of avian coronavirus infectious bronchitis virus. Vaccine 8, 605–608.

Lai, M.M., Baric, R.S., Makino, S., Keck, J.G., Egbert, J., Leibowitz, J.L., Stohlman, S.A., 1985. Recombination between nonsegmented RNA genomes of murine coronaviruses. J. Virol. 56, 449–456.

Lee, C.W., Jackwood, M.W., 2000. Evidence of genetic diversity generated by recombination among avian coronavirus IBV. Arch. Virol. 145, 2135–2148.

Li, K., Chen, Z., Plagemann, P., 1999. High frequency homologous genetic recombination of an arterivirus, lactate dehydrogenase virus, in mice and evolution of neuropathogenic variants. Virology 285, 73–83.

Limsuwan, C., 1991. Handbook for Cultivation of Black Tiger Prawns. Tamsetakit Co., Ltd., Bangkok (in Thai).

Lole, K.S., Bollinger, R.C., Paranjape, R.S., Gadkari, D., Kulkarni, S.S., Novak, N.G., Ingersoll, R., Sheppard, H.W., Ray, S.C., 1999. Full-length human immunodeficiency virus type 1 genomes from subtype C-infected seroconverters in India, with evidence of intersubtype recombination. J. Virol. 73, 152–160.

Luytjes, W., Bredenbeek, P.J., Noten, A.F., Horzinek, M.C., Spaan, W.J., 1988. Sequence of mouse hepatitis virus A59 mRNA 2: indications of RNA recombination between coronaviruses and influenza C virus. Virology 166, 415–422.

Makino, S., Keck, J.G., Stohlman, S.A., Lai, M.M., 1986. High-frequency RNA recombination of murine coronaviruses. J. Virol. 57, 729–737.

Manivannan, S., Otta, S.K., Karunasagar, I., Karunasagar, I., 2002. Multiple viral infection in *Penaeus monodon* shrimp postlarvae in an Indian hatchery. Dis. Aquat. Org. 48, 233–236.

Molenkamp, R., Greve, S., Spaan, W.J.M., Snijder, E.J., 2000. Efficient homologous RNA recombination and requirement for an open reading frame during replication of equine arteritis virus defective interfering RNAs. J. Virol. 74, 9062–9070.

Monci, F., Sánchez-Campos, S., Navas-Castillo, J., Moriones, E., 2002. A natural recombinant between the geminiviruses tomato yellow leaf curl Sardinia virus and tomato yellow leaf curl virus exhibits a novel pathogenic phenotype and is becoming prevalent in Spanish populations. Virology 303, 317–326.

Moonan, F., Molina, J., Mirkov, T.E., 2000. Sugarcane yellow leaf virus: an emerging virus that has evolved by recombination between luteoviral and poleroviral ancestors. Virology 269, 156–171.

Motokawa, K., Hohdatsu, T., Aizawa, C., Koyama, H., Hashimoto, H., 1995. Molecular cloning and sequence determination of the peplomer protein gene of feline infectious peritonitis virus type I. Arch. Virol. 140, 469–480.

Nagy, P.D., Ogiela, C., Bujarski, J.J., 1999. Mapping sequences active in homologous RNA recombination in brome mosaic virus: prediction of recombination hot spots. Virology 254, 92–104.

Natividad, K.T., Magbanua, F., Migo, V.P., Alfafara, C.G., Albaladejo, J., Nadala, E.C.B., Loh, P.C., Tapay, L.M., 2002. Prevalence of yellow head virus in cultured black tiger shrimp (*Penaeus monodon* Fabricius) from selected shrimp farms in the Philippines. In: Lavilla-Pitogo, C.R., Cruz-Lacierda, E.R. (Eds.), Diseases in Asian Aquaculture IV. Fish Health Section. Asian Fisheries Society, Manila, pp. 45–55.

Natividad, K.T., Migo, V.P., Albaladejo, J., Magbanua, F., Noruma, N., Matsumura, M., 2006. Simultaneous PCR detection of two shrimp viruses (WSSV and MBV) in postlarvae of *Penaeus monodon* in the Philippines. Aquaculture 257, 142–149.

Pasharawipas, T., Flegel, T.W., Sriurairatana, S., Morrison, D.J., 1997. Latent yellow-head infections in *Penaeus monodon* an implications regarding disease resistance or tolerance. In: Flegel, T.W., Menasveta, P., Paisarnat, S. (Eds.), Shrimp Biotechnology in Thailand. National Center for Genetic Engineering and Biotechnology, Bangkok, pp. 45–53.

Rambaut, A., Grassly, N.C., 1997. Seq-Gen: an application for the Monto Carlo simulation of DNA sequence evolution along phylogenetic trees. Comput. Appl. Biosci. 13, 235–238.

Shapka, N., Nagy, P.D., 2004. The AU-rich RNA recombination hot spot sequence of Brome mosaic virus is functional in tombusviruses: implications for the mechanism of RNA recombination. J. Virol. 78, 2288–2300.

Sittidilokratna, N., Hodgson, R.A.J., Cowley, J.A., Jitrapakdee, S., Boonsaeng, V., Panyim, S., Walker, P.J., 2002. Complete ORF1b gene sequence indicates yellow head virus is an invertebrate nidovirus. Dis. Aquat. Org. 50, 87–93.

Sittidilokratna, N., Phetchampai, N., Boonsaeng, V., Walker, P.J., 2006. Structural and antigenic analysis of the yellow head virus nucleocapsid protein p20. Virus Res. 116, 21–29.

Sittidilokratna, N., Dangtip, S.N., Cowley, J.A., Walker, P.J., 2008. RNA transcription analysis and completion of the genome sequence of yellow head nidovirus. Virus Res. 136, 157–165.

Sittidilokratna, N., Charoonroj Chotwiwatthanakun, C., Wijegoonawardane, P.K.M., Unajak, S., Boonnad, A., Wangnai, W., Jitrapakdee, S., Cowley, J.A., Walker, P.J., 2009. A virulent isolate of yellow head nidovirus contains a deformed envelope glycoprotein gp116. Virology 384, 192–200.

Smits, S.L., Lavazza, A., Matiz, K., Horzinek, M.C., Koopmans, M.P., de Groot, R.J., 2003. Phylogenetic and evolutionary relationship among torovirus field variants: evidence for multiple intertypic recombination events. J. Virol. 77, 9567–9577.

Snijder, E.J., den Boon, J.A., Horzinek, M.C., Spaan, W.J., 1991. Comparison of the genome organization of toro- and coronaviruses: evidence for two nonhomologous RNA recombination events during Berne virus evolution. Virology 180, 448–452.

Soowannayan, C., Flegel, T.W., Sithigorngul, P., Slater, J., Hyatt, A., Crameri, S., Wise, T., Crane, M.St.J., Cowley, J.A., McCulloch, R., Walker, P.J., 2003. Detection and differentiation of yellow head complex viruses using monoclonal antibodies. Dis. Aquat. Org. 57, 193–200.

Spann, K.M., Vickers, J.E., Lester, R.J.G., 1995. Lymphoid organ virus of *Penaeus monodon* from Australia. Dis. Aquat. Org. 23, 127–134.

Spann, K.M., Cowley, J.A., Walker, P.J., Lester, R.J.G., 1997. A yellow-head-like virus from *Penaeus monodon* cultured in Australia. Dis. Aquat. Org. 31, 169–179.

Spann, K.M., Donaldson, A.R., East, I.J., Cowley, J.A., Walker, P.J., 2000. Differences in the susceptibility of four penaeid prawn species to gill-associated virus (GAV). Dis. Aquat. Org. 42, 221–225.

Spann, K.M., McCulloch, R.J., Cowley, J.A., East, I.J., Walker, P.J., 2003. Detection of gill-associated virus (GAV) by *in situ* hybridization during acute and chronic infections of *Penaeus monodon* and *P. esculentus* shrimp. Dis. Aquat. Org. 56, 1–10.

Thompson, J.D., Higgins, D.G., Gibson, T.J., 1994. ClustalW — improving the sensitivity of progressive multiple sequence alignment through sequence weighting, position-specific gap penalties and weight matrix choice. Nucleic Acids Res. 22, 4673–4680.

van Vugt, J.J., Storgaard, T., Oleksiewicz, M.B., Bøtner, A., 2001. High frequency RNA recombination in porcine reproductive and respiratory syndrome virus occurs preferentially between parental sequences with high similarity. J. Gen. Virol. 82, 2615–2620.

Walker, P.J., Cowley, J.A., Spann, K.M., Hodgson, R.A.J., Hall, M.R., Withychumnarnkul, B., 2001. Yellow head complex viruses: transmission cycles and topographical distribution in the Asia-Pacific region. In: Browdy, C.L., Jory, D.E. (Eds.), The New Wave: Proceedings of the Special Session on Sustainable Shrimp Culture, Aquaculture 2001. The World Aquaculture Society, Baton Rouge, La., pp. 292–302.

Walker, P.J., Flegel, T.W., Boonsaeng, V., Lightner, D.V., Tang, K., Loh, P.C., Chang, P.S., Bonami, J.R., Cowley, J.A., Snijder, E., Enjuanes, L., 2004. *Roniviridae*. In: Fauquet, C.M., Mayo, M.A., Maniloff, J., Desselberger, U., Ball, L.A. (Eds.), Virus Taxonomy, Eighth Report of the ICTV. Elsevier/Academic Press, London, pp. 973–977.

Walker, P.J., Mohan, C.V., 2009. Viral disease emergence in shrimp aquaculture: origins, impact and the effectiveness of health management strategies. Rev. Aquacul. 125–154.

Wang, L., Junker, D., Collisson, E.W., 1993. Evidence of natural recombination within the S1 gene of infectious bronchitis virus. Virology 192, 710–716.

Wijegoonawardane, P.K.M., Cowley, J.A., Phan, T., Hodgson, R.A.J, Nielsen, L., Kiatpathomchai, W., Walker, P.J., 2008a. Genetic diversity in the yellow head nidovirus complex. Virology 380, 213–225.

Wijegoonawardane, P.K.M., Cowley, J.A., Walker, P.J., 2008b. Consensus RT-nested PCR detection of yellow head complex genotypes in penaeid shrimp. J. Virol. Meth. 153, 168–175.

Wongteerasupaya, C., Tongcheua, W., Boonsaeng, V., Panyim, S., Tassanakajon, A., Withyachumnarnkul, B., Flegel, T.W., 1997. Detection of yellow-head virus of *Penaeus monodon* by RT-PCR amplification. Dis. Aquat. Org. 31, 181–186.

Woo, P.C.Y., Lau, S.K.P., Yip, C.C.Y., Huang, Y., Tsoi, H.W., Chan, K.H., Yuen, K.Y., 2006. Comparative analysis of 22 coronavirus HKU1 genomes reveals a novel genotype and evidence of natural recombination in coronavirus HKU1. J. Virol. 80, 7136–7145.

Worobey, M., Holmes, E.C., 1999. Evolutionary aspects of recombination in RNA viruses. J. Gen. Virol. 80, 2535–2543.

Yuen, S., Nelsen, C.J., Murtaugh, M.P., Schmitt, B.J., Faaberg, K.S., 1999. Recombination between North American strains of porcine reproductive and respiratory syndrome virus. Virus Res. 61, 87–97.